

# Modeling the Heating of Biological Tissue based on the Hyperbolic Heat Transfer Equation

M. M. Tung<sup>a,\*</sup>, M. Trujillo<sup>b</sup>, J.A. López Molina<sup>b</sup>,  
M.J. Rivera<sup>b</sup>, and E.J. Berjano<sup>c</sup>

<sup>a</sup>*Instituto de Matemática Multidisciplinar*

<sup>b</sup>*Instituto de Matemática Pura y Aplicada*

<sup>c</sup>*Instituto de Investigación e Innovación en Bioingeniería*

*Universidad Politécnica de Valencia, Valencia, Spain*

## Abstract

In modern surgery, a multitude of minimally intrusive operational techniques are used which are based on the punctual heating of target zones of human tissue via laser or radio-frequency currents. Traditionally, these processes are modeled by the bioheat equation introduced by Pennes, who considers Fourier's theory of heat conduction. We present an alternative and more realistic model established by the hyperbolic equation of heat transfer. To demonstrate some features and advantages of our proposed method, we apply the obtained results to different types of tissue heating with high energy fluxes, in particular radiofrequency heating and pulsed laser treatment of the cornea to correct refractive errors. Hopefully, the results of our approach help to refine surgical interventions in this novel field of medical treatment.

*Key words:* heat models, Fourier heat equation, parabolic heat equation, bioheat equation, radiofrequency surgery, laser ablation

\* corresponding author

Email addresses: mtung@imm.upv.es (M. M. Tung), matruggui@mat.upv.es  
(M. Trujillo), jalopez@mat.upv.es (J.A. López Molina), mjrivera@mat.upv.es  
(M.J. Rivera), eberjano@eln.upv.es (E.J. Berjano).

<sup>1</sup> This work received financial support from the Spanish “Plan Nacional de Investigación Científica, Desarrollo e Innovación Tecnológica del Ministerio de Educación y Ciencia” (TEC 2005-04199/TCM) and from the MEC and FEDER Project MTM2007-64222.

## 1 INTRODUCTION

Presently, modern surgery has at its disposal a great variety of different surgical techniques to heat biological tissue in a localized and safe way. All these techniques are based on specific applicators, *i.e.* devices which extract (cryosurgery) or introduce heat (laser, radiofrequency current, microwave or ultrasound treatments). Theoretical heat modeling is a very cheap and fast methodology to study the thermal performance of these applicators. In fact, a lot of previous work has been conducted to model these procedures by using the bioheat equation as governing equation (see [1], and references therein). This equation is based on the classical Fourier theory of heat conduction and is widely used for modeling the heating of biological tissue. Nevertheless, it has been hypothesized that for heat transfers on very small time scales the classical model will fail, and an alternative thermal wave theory with a finite thermal propagation speed could be more suitable to describe these phenomena.

For the aforementioned reasons, we are lead to modeling the surgical heating of biological tissue by means of the hyperbolic heat transfer equation, and then compare these alternative results with those obtained from the standard Fourier theory (implying the parabolic heat transfer equation).

In summary, the main theme of this work is to present in depth the mathematical and physical background for a general discussion of heat models related to heating of biological tissue by means of energy applicators, and then, in particular, point out the physical differences between the classical Fourier theory and the hyperbolic wave theory. Moreover, as an illustrative example, we give some numerical results of the analytical modeling for radiofrequency heating (*RFH*) and for laser heating, each applied to the cornea in order to correct refractive errors. Both surgical techniques have in common that they may involve high heat transfers during very short exposure times.

This paper is organized as follows. In Sec. 2 we will set up the mathematical groundwork for heat models related to *RFH* and laser heating with a special emphasis on parabolic and hyperbolic heat models. Then, in Sec. 3 we present the results for typical laser and *RFH* interventions in order to substantiate the physical discrepancies between both heat models in concrete examples. We will also comment on the domain of applicability of both theories and their main features. Finally, Sec. 4 will present the conclusions and give an outlook on interesting future work.

## 2 HYPERBOLIC VERSUS PARABOLIC HEAT MODELS

The most fundamental relation to model heat transfer is the generally valid, *i.e.* model-independent, equation for thermal current conservation with a given internal heat source  $S(\mathbf{x}, t)$ :

$$\nabla \cdot \mathbf{q}(\mathbf{x}, t) + \frac{k}{\alpha} \frac{\partial T}{\partial t}(\mathbf{x}, t) = S(\mathbf{x}, t). \quad (1)$$

Here,  $\mathbf{q}(\mathbf{x}, t)$  denotes the thermal flux and  $T(\mathbf{x}, t)$  is the temperature at point  $\mathbf{x} \in D$  in the domain  $D \subset \mathbb{R}^3$  at time  $t \in \mathbb{R}_+$ . As usual, thermal conductivity is denoted by  $k > 0$  and diffusivity by  $\alpha = k/\rho c$ , where  $\rho c$  is the volumetric heat capacity, being  $\rho$  the density and  $c$  the specific heat of the material under consideration. Fig. 1 gives a schematic view of thermal current conservation.

Fourier's law of heat conduction [2] constitutes the foundation of all classical heat models. It proposes that the heat flux  $\mathbf{q}(\mathbf{x}, t)$  is proportional to the negative of the temperature gradient (see Fig. 2):

$$\mathbf{q}(\mathbf{x}, t) = -k \nabla T(\mathbf{x}, t). \quad (2)$$

However, in this relation temporal changes instantaneously affect heat flux and temperature gradient. As an immediate consequence any perturbations in classical heat models are propagated with infinite speed.

Assuming that thermal current conservation (1) and Fourier's law (2) hold, directly yields the classical, *i.e.* parabolic heat transfer equation (*PHT*E) with heat sources:

$$-\Delta T(\mathbf{x}, t) + \frac{1}{\alpha} \frac{\partial T}{\partial t}(\mathbf{x}, t) = \frac{1}{k} S(\mathbf{x}, t). \quad (3)$$

The standard bioheat equation was introduced by Pennes [3] and is based on the parabolic heat transfer model, identifying the following explicit contributions for the heat sources in a biological system

$$S(\mathbf{x}, t) = S_s(\mathbf{x}, t) + S_p(\mathbf{x}, t) + S_m(\mathbf{x}, t), \quad (4)$$

where the subindex  $s$  denotes a surgical heat source (*e.g.* laser or radiofrequency treatment),  $p$  refers to blood perfusion, and  $m$  to any source related to metabolic activity.

With the advancement of modern surgery, medical treatments involve progressively smaller time scales and higher energy fluxes. For example, for ra-

diofrequency and laser surgery *PHT*E models could become inappropriate. The reason is that on small time scales  $t \in [0, \tau]$ , with a sufficiently small value for  $\tau > 0$ , thermal equilibrium of an extended physical system simply can not be reached. This contradicts the classical model, where all elements of the thermodynamic system interact with no delay through infinite thermal speed. It is to be expected that such theories implying infinite speed of perturbations in the heated medium and more realistic wave theories with finite speeds differ considerably in their predictions.

A modified version of Fourier's law (2) uses a non-vanishing relaxation time  $\tau$  in the dissipative process. This parameter may be interpreted as the finite time necessary for the dissipative flow to relax to its steady thermodynamic value. The simplest generalization for finite speeds leads to Cattaneo-Vernotte's equation [4,5]:

$$\mathbf{q}(\mathbf{x}, t + \tau) = -k \nabla T(\mathbf{x}, t). \quad (5)$$

Note that the classical Fourier law is still included as a special limiting case, taking the limit of zero relaxation time for the heat fluxes. In general, however, there is an inertial or retardation term which delays any changes in the temperature gradient to be transferred to the heat flux. This can also be seen for small relaxation intervals  $\tau$ , which yields the expression

$$\mathbf{q}(\mathbf{x}, t) + \tau \frac{\partial \mathbf{q}}{\partial t}(\mathbf{x}, t) = -k \nabla T(\mathbf{x}, t). \quad (6)$$

Although it appears at first sight that Eq. (6) is an expansion which only holds approximately for small relaxation intervals  $\tau$ , by considering entropy arguments Özışik and Tzou have shown that Eq. (6) is also valid on a macroscopic scale [6].

By combining the heat transfer model (6) with current conservation (1), one directly obtains the hyperbolic heat transfer equation (*HHT*E) with heat sources:

$$-\Delta T(\mathbf{x}, t) + \frac{1}{\alpha} \left( \frac{\partial T}{\partial t}(\mathbf{x}, t) + \tau \frac{\partial^2 T}{\partial t^2}(\mathbf{x}, t) \right) = \frac{1}{k} \left( S(\mathbf{x}, t) + \tau \frac{\partial S}{\partial t}(\mathbf{x}, t) \right). \quad (7)$$

For zero relaxation the hyperbolic heat equation obviously reduces to the classical model. An essential feature of Eq. (7) is the second-order time derivative with coefficient  $\tau > 0$ , which gives rise to wave properties of the equation, and therefore implies finite thermal propagation speeds. This can easily be seen by considering forwardly propagating waves which provide solutions for Eq. (7)

of the form

$$T_{\text{wave}} := e^{i(\mathbf{k} \cdot \mathbf{x} - \omega t)} f(\mathbf{x} - \mathbf{v}t), \quad (8)$$

where  $\mathbf{k}$  is the usual wave propagation vector and  $\omega$  the corresponding frequency. This approach is somehow analogous to the analysis of the *telegraph equation*, which describes the propagation of electromagnetic waves in conducting media [7,8]. Note that in the present case, however, a term proportional to  $T(\mathbf{x}, t)$  is absent on the left-hand side of Eq. (7).

By following the procedure of Ref. [7] and substituting Eq. (8) into Eq. (7) for sourceless heat transfer, then requiring that the real-numbered factor multiplying with  $\Delta f$  has to be zero, one directly obtains for the thermal propagation speed

$$v = \sqrt{\frac{\alpha}{\tau}} \quad \text{with} \quad \tau > 0. \quad (9)$$

From this it becomes evident that for vanishing relaxation times  $\tau$  and constant diffusivity  $\alpha > 0$ , the propagation speed tends to infinity. As indicated before, but seen from a different perspective, in this limiting case the hyperbolic model reduces again to the standard Fourier theory.

One further distinctive feature of the *HHTE* model is observed by representing the hyperbolic heat flux equation (6) in integral form [6]

$$\mathbf{q}(\mathbf{x}, t) = -\frac{k}{\tau} e^{-t/\tau} \int_0^t e^{s/\tau} \nabla T(\mathbf{x}, s) ds. \quad (10)$$

Note that Eq. (10) shows that  $\mathbf{q}(\mathbf{x}, t)$  depends on the full history of the temperature gradient within the time interval  $[0, t]$ , something which is entirely absent in the much simpler expression for the Fourier flux in Eq. (2).

Exhibiting these features, the hyperbolic heat transfer model with its finite thermal propagation appears to provide an ideal framework to describe surgical interventions such as laser ablation (a procedure named as laser thermo-keratoplasty, or short *LTK*) and *RFH* of the cornea (*CK*, conductive keratoplasty), which use very short and high-energetic pulsations (typical time periods are 200  $\mu\text{s}$  and 50  $\mu\text{s}$ , respectively). Therefore, in the following section, we will focus on applications of heat models in surgical techniques, in particular *RFH* and laser surgery applied to the cornea, and thereby develop a realistic model for the heating of biological tissue by employing the *HHTE* as previously derived in Eq. (7).

### 3 SURGICAL APPLICATIONS IN HEAT MODELS

There exist numerous processes in which great amounts of heat are applied to materials in very short exposure times. This section will focus on the modeling of heating biological tissue as it occurs during medical intervention with surgical radiofrequency or laser devices to the cornea.

Laser heating is a process which implies tissue heating caused by absorbing the optical energy of a high-energy laser beam (*LTK*). On the other hand, radiofrequency heating (*RFH*) is ultimately based on Ohm's law, which states that currents flowing through a resistor generate heat. It is essentially ionic motion in the tissue which will provoke biological heating aimed at producing any medical effects. Both are surgical techniques which may not only involve small time scales but also high energy fluxes, which makes them an important group of applications in which differences between parabolic and hyperbolic models could have great effects.

As we have previously mentioned in Sec. 2, these type of processes represent non-equilibrium processes on small time scales (*i.e.* compared to the relaxation time  $\tau$ ), since the system requires considerably more time to reach the equilibrium state after the initial thermal energy input. For this reason, *PHT*E models, with their infinite thermal propagation speed, may not provide an appropriate description for the underlying physical structure, and it may be necessary to rely on *HHT*E models instead.

#### 3.1 *Laser Heating*

Among the many surgical procedures in which laser heating is employed, we focus our attention on corneal laser heating, also referred to as laser thermo-keratoplasty (*LTK*) [9].

In the case of laser heating, we consider a theoretical model consisting of a semi-infinite fragment of homogeneous isotropic biological tissue in which the laser beam falls on the entire tissue surface. Fig. 3 depicts the chosen model geometry, in which we consider a one-dimensional model with the  $x$ -axis parallel to the direction of the incident laser beam. Above the surface, for  $x < 0$ , free thermal convection is supposed to cool the tissue surface.

As we want to study the problem from the point of view of the *HHT*E model, we have to start off from the governing equation provided by Eq. (7). For this one-dimensional laser heating model, we have to solve the corresponding heat transfer equation for penetration depth  $x$  including the appropriate heat-source term and boundary conditions.

Neglecting blood perfusion and metabolic activity in Eq. (4), and hence  $S_p = S_m = 0$ , the heat source  $S(x, t)$  will only have contributions from  $S_s(x, t)$ . This surgical source should be obtained from the Beer-Lambert law, which empirically states that for radiation the intensity decreases exponentially with penetration depth. Including a factor with the temporal dependence to model an energy pulse of duration  $\Delta t$ , this yields

$$S(x, t) = (1 - R) b E_0 e^{-bx} [H(t) - H(t - \Delta t)], \quad (11)$$

where  $R$  denotes the dimensionless Fresnel surface reflectance,  $b$  is the absorption coefficient, and  $E_0$  is the incident energy flux at the tissue surface [9]. As usual,  $H(t)$  denotes the Heaviside function. After combining Eqs. (7) and (11), the final form of the governing equation is

$$\begin{aligned} -\frac{\partial^2 T}{\partial x^2}(x, t) + \frac{1}{\alpha} \left( \frac{\partial T}{\partial t}(x, t) + \tau \frac{\partial^2 T}{\partial t^2}(x, t) \right) = \\ (1 - R) \frac{b E_0}{k} e^{-bx} [H(t) - H(t - \Delta t) + \tau (\delta(t) - \delta(t - \Delta t))], \end{aligned} \quad (12)$$

where  $\delta(t)$  is the Dirac delta function.

The corresponding initial boundary conditions are given by

$$\begin{aligned} T(x, 0) = T_0, & \quad \frac{\partial T}{\partial t}(x, 0) = 0 \quad \forall x > 0 \\ \lim_{x \rightarrow \infty} T(x, t) = T_0 & \quad \forall t > 0 \\ \frac{\partial T}{\partial x}(0, t) = \frac{h}{k} \left( \tau \frac{\partial T}{\partial t}(0, t) + T(0, t) - T_a \right) & \quad \forall t > 0 \end{aligned} \quad (13)$$

where  $T_0$  is the initial temperature and  $T_a$  is the ambient temperature. Furthermore,  $h > 0$  is the thermal convection constant at the interface tissue given by Newton's law of cooling, which states that the convective flux of an object is proportional to the difference between its own temperature  $T_0$  and the ambient temperature  $T_a$ :

$$q(0, t) = h [T_a - T(0, t)]. \quad (14)$$

Since at the interface tissue with  $x = 0$  the heat flux is given by the Newton's law of cooling, the last condition of Eq. (13) is obtained by imposing this law onto the relation for the hyperbolic heat flux Eq. (10) (see also [6]).

The explicit analytical solution of this problem has been obtained in Ref. [10] and is mainly based on the use of Laplace transforms. It also contains for com-

thermal properties			
density $\rho$ [kgm <sup>-3</sup> ]	conductivity $k$ [Wm <sup>-1</sup> K <sup>-1</sup> ]	diffusivity $\alpha$ [m <sup>2</sup> s <sup>-1</sup> ]	convection $h$ [Wm <sup>-2</sup> K <sup>-1</sup> ]
1060	0.556	$1.3695 \cdot 10^{-7}$	20
optical properties			
Fresnel reflectance $R$		absorption coefficient $b$ [m <sup>-1</sup> ]	
0.024		2000	

Table 1  
Thermal and optical properties of the human cornea.

parison the fully analytical *PHTE* solution as an application to the thermo-keratoplasty technique. For the numerical estimates, well-established thermal and optical properties of the cornea were used. All essential physical constants for the model are summarized in Tab. 3.1.

Figure 4 shows the numerical estimates for temperatures at various tissue penetration depths obtained as a function of time [10]. This figure represents the hyperbolic (solid line) and parabolic (dashed line) temperature evolution at the four locations  $x = 0.01, 0.1, 0.5$  and  $1$  mm for the thermokeratoplasty technique.

We can mainly find two differences between both solutions:

Firstly, according to the parabolic model, for the values  $x = 0.01$  and  $0.1$  mm the maximum temperature has already been reached and is steadily decreasing. For  $x = 0.5$  and  $1$  mm, the maximum temperature has not yet been reached and is initially increasing. For the *HHTE* predictions, we observe that for all penetration depths in some part of the plot (or the entire plot) the temperature is increasing. The great differences in temperatures between both models (overall at positions closer to the surface  $x = 0.01$  and  $0.1$  mm) is even more important when the energy application is pulsed, since in every new pulse the difference between the initial temperature could become greater and greater.

Secondly, we can confirm that the behavior of both solutions is very different. At values  $x = 0.01$  and  $0.1$  mm, we notice a delay in the abrupt temperature drop associated with switching off the laser beam. This delay is related to the finite thermal propagation speed in the *HHTE* model. Using in Eq. (9) the numerical value for diffusivity (*viz.* Tab. 3.1) and for the relaxation time

$\tau = 10$  s predicts

$$v = 0.117 \frac{\text{mm}}{\text{s}} \quad (15)$$

for the speed of these steps, which exactly agrees with the known finite speed of the thermal wave in the cornea [10]. This fact demonstrates the wave character of the *HHTE* model. For depths  $x = 0.5$  and  $1$  mm, however, these drops are not observed, because they occur outside the range of the time interval considered.

### 3.2 Radiofrequency Heating

Radiofrequency heating (*RFH*) is a surgical procedure broadly employed in many clinical areas such as the elimination of cardiac arrhythmias, the destruction of tumors, the treatment of gastroesophageal reflux disease and the heating of the cornea for refractive surgery [11]. In the remainder of this section we will focus on a model of the corneal *RFH* treatment.

The schematic diagram of the model geometry is shown in Fig. 5. Here, a spherical electrode of radius  $r_0$  is completely embedded and in close contact with the biological tissue, which has infinite dimension. In this case, we can also use a one-dimensional model ( $r$  being the spatial variable), since the geometry under consideration displays radial symmetry.

Again, assuming  $S_p = S_m = 0$  in the bioheat equation (4), the governing equation results from the combination of Eq. (7) and the explicit form of the (surgical) heat source  $S(r, t)$  which in the case of *RFH* is a product of a radial [12] and a temporal part

$$S(r, t) = S(r) H(t) = \frac{Pr_0}{4\pi r^4} H(t), \quad (16)$$

so that the total applied power outside of the electrode is

$$P = \int_{\text{shell}} S(r) dV = \oint d\Omega \int_{r_0}^{\infty} r^2 S(r) dr, \quad (17)$$

where  $\Omega$  is the usual solid angle subtended by a surface. Thus, the power (flux) per unit solid angle,  $dP/d\Omega$ , satisfies the usual  $1/r^2$  intensity law. Note that  $H(t)$  is included to model a non-pulsed source. As a result, for the corneal

*RFH* the governing equation and the boundary conditions are:

$$\begin{aligned}
-\frac{1}{r^2} \frac{\partial}{\partial r} \left( r^2 \frac{\partial T}{\partial r}(r, t) \right) + \frac{1}{\alpha} \left( \frac{\partial T}{\partial t}(r, t) + \tau \frac{\partial^2 T}{\partial t^2}(r, t) \right) &= \frac{Pr_0}{4\pi k r^4} [H(t) + \tau \delta(t)] \\
T(r, 0) = T_0, \quad \frac{\partial T}{\partial t}(r, 0) = 0 \quad \forall r > r_0 \\
\lim_{r \rightarrow \infty} T(r, t) = T_0 \quad \forall t > 0 \\
\frac{\partial^2 T}{\partial t^2}(r_0, t) + \frac{1}{\tau} \frac{\partial T}{\partial t}(r_0, t) &= \frac{3k}{\rho_0 c_0 r_0 \tau} \frac{\partial T}{\partial r}(r_0, t) \quad \forall t > 0
\end{aligned} \tag{18}$$

The last condition in Eqs. (18) contains the density and specific heat of the electrode (where  $r \leq r_0$ ), given by  $\rho_0 = 21500 \text{ kg m}^{-3}$  and  $c_0 = 132 \text{ J kg}^{-1}\text{K}^{-1}$ , respectively. This condition is based on the fact that in the interior and on the surface of the spherical electrode it must hold

$$\nabla \cdot \mathbf{q}(r, t) + \rho_0 c_0 \frac{\partial T}{\partial t}(r, t) \Big|_{r \leq r_0} = 0, \tag{19}$$

which just states that the heat flux  $\mathbf{q}$  spreading into the biological tissue is due to the change of the thermal energy content of the electrode. Applying Gauss' law to Eq. (19) and integrating over the entire volume  $r \leq r_0$  yields

$$\oint \mathbf{q}(r, t) \cdot \hat{\mathbf{e}}_r r_0^2 d\Omega + \rho_0 c_0 \frac{4\pi r_0^3}{3} \frac{\partial T}{\partial t}(r, t) = 0, \tag{20}$$

where we have assumed that the electrode has relatively small radius and sufficiently high thermal conductivity, which makes the electrode act like a punctual heat source. In the derivation of Eq. (20), this justifies taking  $\rho_0 c_0$  to be constant and pulling  $\partial T / \partial t$  out of the volume integral.

Finally, by substituting the expression for the hyperbolic heat flux Eq. (10) into Eq. (20) and using  $\nabla T \cdot \hat{\mathbf{e}}_r = \partial T / \partial r$ , where  $\hat{\mathbf{e}}_r$  is the usual radial unit vector, one readily obtains the last condition for the electrode in Eqs. (18).

The analytical solution of this problem and the corresponding *PHTHE* solution have been obtained in Ref. [13] as an application for corneal *RFH*. We have visualized the data generated from Ref. [14] in Fig. 6 in order to discuss the main characteristics of the model. Figure 6 represents the hyperbolic (solid lines) and parabolic (dashed lines) temperature profiles along the radial axis for the times  $t = 10, 30$  and  $50 \text{ ms}$ . Similar to the laser-heating case, for small times and locations near the electrode surface the temperatures from the *HHTHE* are greater than from the *PHTHE*. This fact also becomes important when instead of a non-pulsed *RFH* application a pulsed power is applied.

Moreover, the presence of pronounced peaks in Fig. 6 reveals the wave character of the *HHTe* model and its prediction of a finite heat conduction speed  $v = \sqrt{\alpha/\tau} \approx 1.17$  mm/s.

## 4 CONCLUSIONS AND OUTLOOK

In this paper, we have outlined the fundamentals and main differences between the parabolic and hyperbolic model of heat conduction. These differences encourage the use of the *HHTe* approach in processes in which great amounts of heat are transferred to any material in very short times. Specifically, laser and radiofrequency heating are two surgical techniques of this type of processes. Through the application of *HHTe* to these surgical techniques, we have shown the main characteristics of this model and its differences with *PHTe* predictions.

At the moment, we are working on the analytical modeling of the hyperbolic bioheat equation including a source term for blood perfusion (*viz.* Eq. (4)). This will be less important for non-perfused tissues (such as the cornea), but relevant for well-perfused organs such as *e.g.* the liver.

On the other hand, we are studying the implications of the hyperbolic heat equation for the case of pulsed *RF* applications. Energy pulses for surgical procedures are being employed in such different areas as conductive keratoplasty (*CK*) and *RFH* to destroy tumors.

However, we are well aware of the restrictions of purely analytical models, mainly due to the lack of mathematical tractability. For this reason, we are planning to develop alternative theoretical models based on numerical techniques (such as finite elements) in order to use the hyperbolic bioheat equation in models with more complicated geometry (more realistic electrode and tissue geometries with irregular boundaries) and also varying thermal characteristics.

## References

- [1] E.J. Berjano, Theoretical modeling for radiofrequency ablation: state-of-the-art and challenges for the future, *BioMedical Engineering OnLine* **5**(24), (2006).
- [2] J.B.J. Fourier, *Théorie analytique de la chaleur*, Firmin Didot, Paris, (1822).
- [3] H.H. Pennes, Analysis of tissue and arterial blood temperatures in the resting human forearm (1948), reprinted in *Journal of Applied Physiology* **85**, 5–34, (1998).

- [4] C. Cattaneo, Sur une forme de l'équation de la chaleur éliminant le paradoxe d'une propagation instantanée, *Les Comptes rendus de l'Académie des sciences* **247**, p. 431, (1958).
- [5] P. Vernotte, Les paradoxes de la théorie continue de l'équation de la chaleur, *Les Comptes rendus de l'Académie des sciences* **246**, p. 178, (1958).
- [6] M.N. Özışık and D.Y. Tzou, On the wave theory in heat conduction, *Journal of Heat Transfer* **116**, 526–535, (1994).
- [7] A. Sommerfeld, *Elektrodynamik*, volume III of *Vorlesungen über Theoretische Physik*, Verlag Harri Deutsch, Frankfurt, (2001).
- [8] W.K.H. Panofsky and M. Phillips, *Classical Electricity and Magnetism*, Addison-Wesley, Reading, (1956).
- [9] F. Manns, D. Borja, J.M. Parel, W. Smiddy and W. Culbertson, Semianalytical thermal model for subablative laser heating of homogeneous nonperfused biological tissue: application to laser thermokeratoplasty, *Journal of Biomedical Optics* **8**(2), 288–297, (2003).
- [10] M. Trujillo, M.J. Rivera, J.A. López Molina and E.J. Berjano, Analytical thermal-optic model for laser heating of biological tissue using the hyperbolic heat transfer equation, submitted to *Mathematical Medicine and Biology*, (2008).
- [11] E.J. Berjano, J.L. Alió and J. Saiz, Modeling for radio-frequency conductive keratoplasty: implications for the maximum temperature reached in the cornea, *Physiological Measurement* **26**(3), 157–72, (2005).
- [12] A. Erez and A. Shitzer, Controlled destruction and temperature distributions in biological tissues subjected to monoactive electrocoagulation, *Journal of Biomechanical Engineering* **102**, 42–49, (1980).
- [13] J.A. López Molina, M.J. Rivera, M. Trujillo and E.J. Berjano, Effect of the thermal wave in radiofrequency ablation modeling: an analytical study, *Physics in Medicine and Biology* **53**(5), 1447–1462, (2008).
- [14] J.A. López Molina, M.J. Rivera, M. Trujillo, F. Burdío, J.L. Lequerica, F. Hornero and E.J. Berjano, Assessment of hyperbolic heat transfer equation in theoretical modeling for radiofrequency heating techniques, *The Open Biomedical Engineering Journal* **2**, 22–27, (2008).

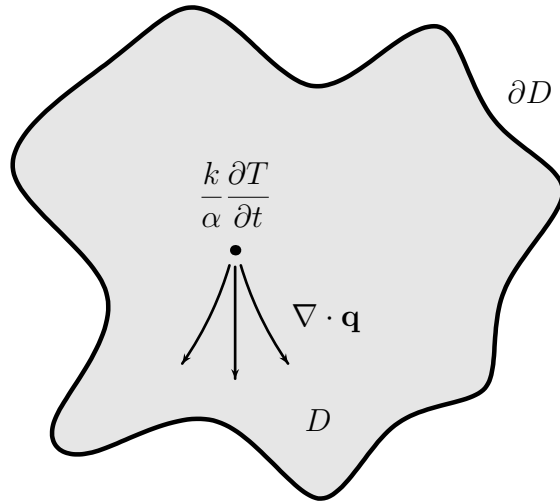


Fig. 1. Schematic view of thermal current conservation. The heat source  $S(\mathbf{x}, t)$  in a physical system ( $D \in \mathbb{R}^3$  simply-connected domain) is related to both, temperature change and divergence of the heat flux  $\mathbf{q}$ . The coefficient  $k/\alpha$  gives the volumetric heat capacity in terms of thermal conductivity and diffusivity.

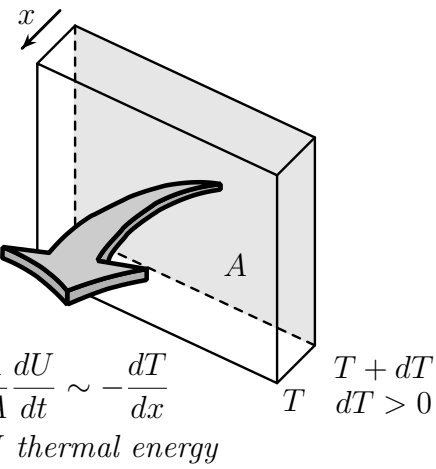


Fig. 2. Fourier's law in differential form, shown for heat transfer through an infinitesimal thin plate with thickness  $dx$  and cross-sectional surface area  $A$ . The corresponding flux, thermal energy per time and area, is proportional to the temperature gradient  $dT/dx$ . The sign indicates that heat flows from  $T + dT$  to  $dT$ .

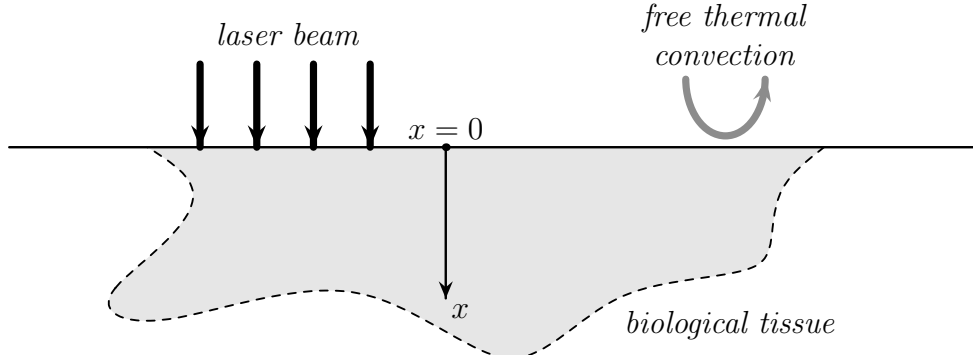


Fig. 3. A schematic view of the model geometry for laser ablation. The laser beam is applied perpendicular to the tissue and defines the  $x$ -axis. The tissue is assumed to take the shape of the half-plane  $x \geq 0$  with free thermal convection above.

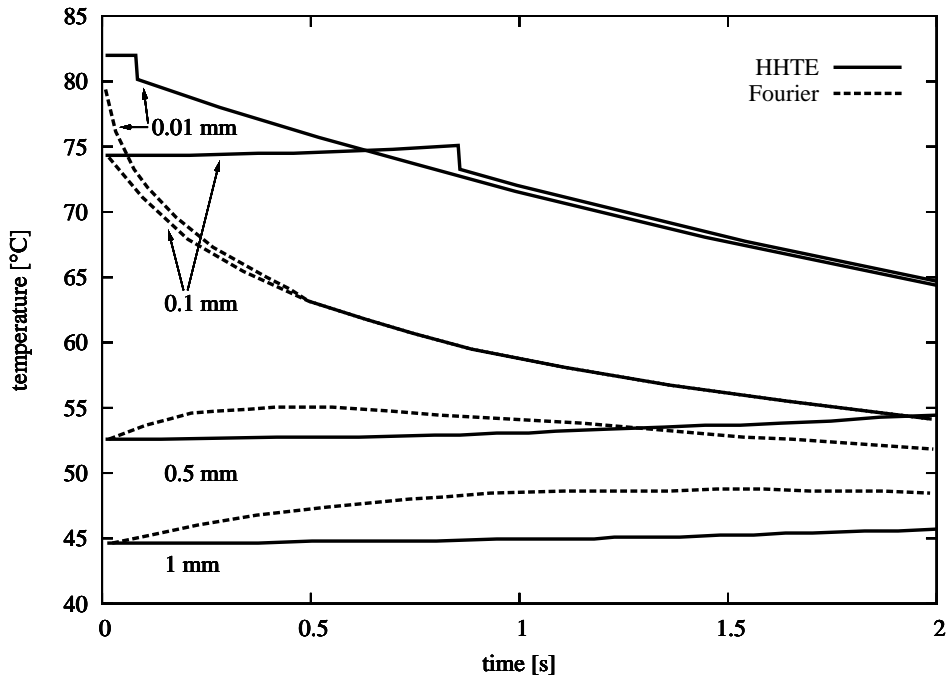


Fig. 4. Temperature profiles for laser heating of the cornea for an initial temperature  $T_0 = 35^\circ\text{C}$  and ambient temperature  $T_a = 20^\circ\text{C}$ . The laser pulse has a duration of  $\Delta t = 200 \mu\text{s}$  with an incident energy flux  $E_0 = 5 \cdot 10^8 \text{ W/m}^2$ . The represented curves for the HHTE (solid lines) and Fourier (dashed lines) model correspond to penetration depths  $x = 0.01, 0.1, 0.5, 1 \text{ mm}$ . The relaxation time is  $\tau = 10 \text{ s}$ .

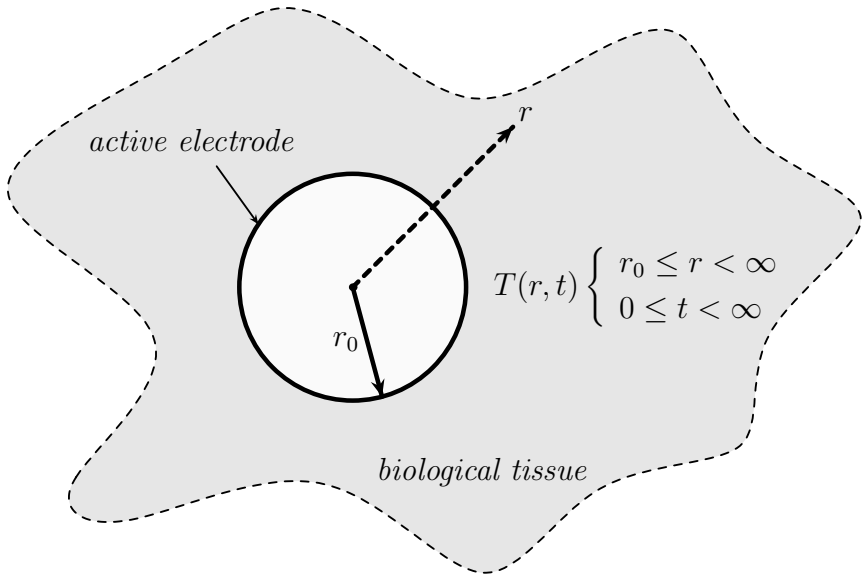


Fig. 5. A graphical sketch of the model geometry for radiofrequency heating, showing the intersection for a spherical electrode. The tip of the active electrode is represented by a sphere of radius  $r_0$ , and the biological tissue extends to infinity. Because of radial symmetry, the problem consists of finding  $T(r, t)$ , imposing specific boundary conditions.

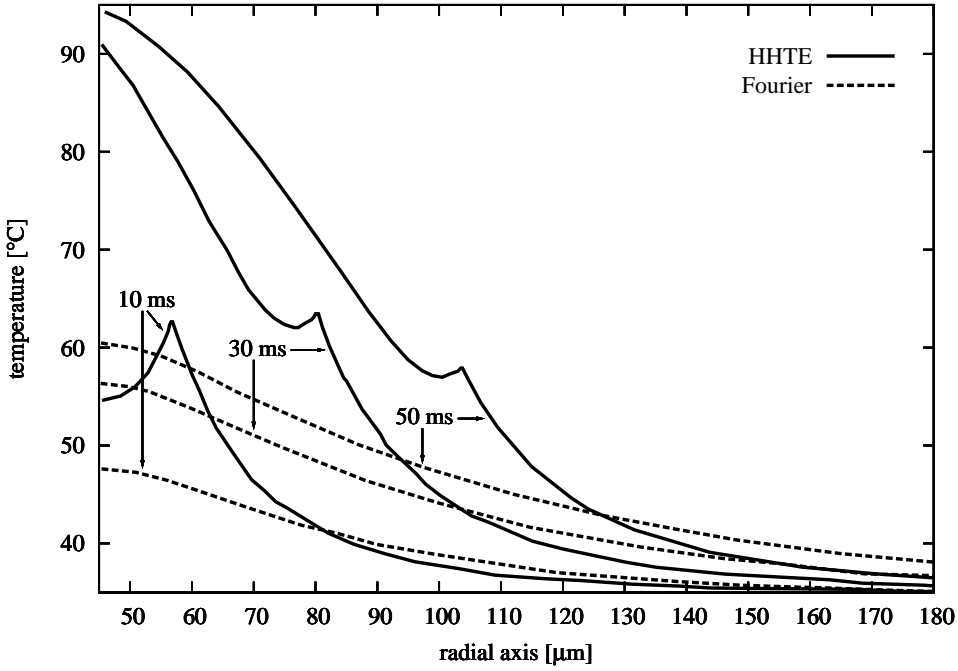


Fig. 6. Temperature distributions for the cornea along the radial axis for three different measured times  $t = 10, 30$ , and  $50$  ms of a non-pulsed RF application with total power  $P = 30$  mW and duration  $\Delta t = 600$  ms. The initial temperature is  $T_0 = 35^\circ\text{C}$  and the electrode radius  $r_0 = 45 \mu\text{m}$ . The relaxation time is taken  $\tau = 0.1\text{s}$ .